User Manual for Hazel and P-Hazel[*]

A. Asensio Ramos

Instituto de Astrofísica de Canarias

38205, La Laguna, Tenerife, Spain

March 9, 2015

---

[*]Hazel (an acronym for HAnle and ZEeman Light) is one of the IAC computer programs for the synthesis and inversion of Stokes profiles resulting from the joint action of the Hanle and Zeeman effects.

Contents

Disclaimer

This software is distributed "as is" and the authors do not take any responsability for possible errors derived from its use by others. Apply it with care and never trust the output without a careful meditation. HAZEL can be freely used provided that its origin is properly acknowledged and the reference Asensio Ramos, Trujillo Bueno & Landi Degl'Innocenti (2008; ApJ 683, 542) is cited and acknowledged in any publication achieved with it. Before using HAZEL we recommend the user to read carefully this paper and the previous one by Trujillo Bueno & Asensio Ramos (2007; ApJ 655, 642). Please, send us bug reports, comments and suggestions of possible improvements. We point out that HAZEL will be improved over the years (e.g., by extending it to more realistic radiative transfer problems), but it is now ready for a number of interesting applications in solar and stellar physics.

1 Introduction

1.1 Description

HAZEL (an acronym for HAnle and ZEeman Light) is a computer program for the synthesis and inversion of Stokes profiles caused by the joint action of atomic level polarization and the Hanle and Zeeman effects. It is based on the quantum theory of spectral line polarization, which takes into account rigorously all the relevant physical mechanisms and ingredients: optical pumping, atomic level polarization, level crossings and repulsions, Zeeman, Paschen-Back and Hanle effects. The code is written in standard Fortran 90. Its parameters are passed using four configuration files that can be manually edited. These configuration files are heavily commented, so that their edition should be an easy task. In any case, two front-ends coded in IDL are given as a part of the distribution in order to facilitate a user-friendly execution of the program. A parallel version of the code using Message Passing Interface (MPI) is also available. This manual considers both distributions.

1.2 Credits

The code has grown since the first version thanks to the suggestions of many people. We thank Rebecca Centeno Elliot, Yukio Katsukawa, Marian Martínez González, Rafael Manso Sainz and Tom Schad for their help on testing the code and proposing (and partially coding, in some cases) some of the options of the code.

2 Uncompressing and compiling Hazel

2.1 Serial version

The package comes in a single compressed file `hazel.tar.gz`. After unpacking with `tar zxvf hazel.tar.gz`, the HAZEL directory will contain the following subdirectories:

1. `Source` contains the Fortran 90 sources and a makefile that can be used to build the binary file.

2. `Run` contains a directory tree structure with the appropriate configuration files to run the code in command line mode.

3. `Widget_Synth` contains all the files that are needed to run the IDL front-end for the synthesis problem.

4. `Widget_Inv` contains all the files that are needed to run the IDL front-end for the inversion problem.

5. `IDL_routines` contains some IDL routines that are needed by the front-ends.

6. `Manual` contains this manual.

The code has been tested on Linux platforms using the Intel Fortran Compiler (`ifort`) and the free GFortran compiler. The source code is in the `Source/` directory. The compilation is performed with the supplied `makefile`. It is quite simple and easy to modify, and contains additional comments about compiling. The default compiler is the `ifort`, although you can use any other compiler through the variable `COMPILER`. In order to obtain the executable file, just type:

```
make all
```

After compiling and linking, the executable is copied to the HAZEL `Run/`, `Widget_Synth/` and `Widget_Inv/` directories. Running the program in the `Run/` directory should produce the correct output depending on the exact form of the input files.

The generated object and module files can be cleaned typing:

```
make clean
```

2.2 Parallel version

The package also decompresses the P-HAZEL directory tree that will contain the following subdirectories:

1. `SourceMPI` contains the Fortran 90 sources and a makefile that can be used to build the binary file.

2. `RunMPI` contains a directory tree structure with the appropriate configuration files to run the code in command line mode.

The source code is in the `SourceMPI/` directory. The compilation depends on the precompiled library NetCDF[1] for reading and writing output files. NetCDF is a standard for platform independent binary files that you need to have installed in your system. The compilation is performed with the supplied `makefile`. It is quite simple and easy to modify, and contains additional comments about compiling. The default compiler is `mpif90`, although you can use any other compiler through the variable `COMPILER`. The variables `NETCDF_INCLUDE` and `NETCDF_LIB` have to point to the `include` and `lib` directories of the NetCDF distribution.

The code makes use of the MPI package for parallelization, so it has to be installed on your system. In order to obtain the executable file (for instance for the Intel compiler), just type:

```
make -f makefile.Intel
```

Modify the `makefile` to point the variables to the correct libraries and include files. After compiling and linking, the executable is copied to the P-HAZEL `RunMPI/` directory, where the code is run. Running the program in the `RunMPI/` directory should produce the correct output depending on the exact form of the input files.

The generated object and module files can be cleaned typing:

---

[1]`http://www.unidata.ucar.edu/software/netcdf/`

```
        make clean
```

The code is run from the `RunMPI` directory. Use your MPI launcher to select the number of processors. For example:

```
mpiexec -n 50 hazel_mpi config_inversion.dat 2000 5000
```

The code admits up to three command line parameters:

- Filename with the main configuration file.

- Starting pixel of the inversion. This is used if you want to rerun the inversion of some pixels.

- Final pixel of the inversion. This is used if you want to rerun the inversion of some pixels.

See §7 for details on the input files.

3   New input file

In previous versions of the code, the code was controlled with four configuration files. The updated version of the code is now controlled by one human-readable configuration file. The code can still be run using the old configuration files but this option will be discontinued in the future so it is advisable to to the shift to this configuration file. The serial code is now run using:

```
./run.py conf.ini
```

and the parallel code is run with

```
./run.py conf.ini nProcessors
```

An example of the file, that is self-explanatory, is:

```
# Hazel configuration File

#####################
# General information
#####################

[Files]
Input model file = 'ATOMS/helium.mod'
File with observations = 'OBSERVATION/test_2comp.prof'
File with inverted profiles = 'test.inversion'
File with inverted parameters = 'test.parameters'

[Working mode]
Action = 'inversion'      # 'synthesis' or 'inversion'
```

```
Verbose = no
Linear system solver = 'LU'          # 'LU' or 'CG'
Stopping volume for DIRECT = 0.001

[General parameters]
Synthesis mode = 'exact'     # 'thin' or 'exact'
Include stimulated emission = yes
Include magnetic field  = yes
Include Paschen-Back effect = yes
Include atomic level polarization = yes
Include magneto-optical effects in the RT = yes
Include stimulated emission in the RT = yes
Multiplet = 10830       # 10830, 5876, 7065, 3889 A
Line-of-sight angles = 0.0, 0.0, 90.0     # theta, chi, gamma deg
Wavelength axis = -3.0, 2.5, 200       # Minimum, maximum and number of grid points


####################
# Synthesis parameters
####################
[Synthesis]
Number of slabs = '1'    # '1' -> single slab, '1+1' -> two slabs with same field, '1+1B
Boundary condition = 4.098e-5, 0.0, 0.0, 0.0      # I0, Q0, U0, V0
a = 0.0
height = 3.0     # Real height if positive, apparent height if negative arcsec
beta = 1.0
ff = 0.0
[[Slab 1]]
B =  0.0 # G
thetaB =  0.0 # deg
chiB =  0.0 # deg
vdopp =  8.0 # km/s
tau =  1.0
vmac =  0.0 # Positive is redshift km/s
[[Slab 2]]
B =  0.0 # G
thetaB =  0.0 # deg
chiB =  0.0 # deg
vdopp =  0.0 # km/s
tau =  0.0
vmac =  0.0 # Positive is redshift km/s


####################
# Ranges for the DIRECT method [min, max]
####################
[Ranges]
```

```
a =   0,0.5
beta =   0.5,2
ff =   0.0,1.0
[[Slab 1]]
B =   800,1100
thetaB =   0,180
chiB =   0,180
vdopp =   2,12
tau =   0.1,2
vmac =   -5,5
[[Slab 2]]
B =   800,1100
thetaB =   0,180
chiB =   0,180
vdopp =   2,12
tau =   0.1,2
vmac =   -5,5


####################
# Parameters to invert
####################
[Inversion]
Iterations in LM = 20
Number of cycles = 4
Inversion modes = 'DIRECT', 'LM', 'DIRECT', 'LM'          # 'DIRECT' for DIRECT algorithm
[[Cycles]]
a =     1, 1, 0, 0
beta = 0, 0, 0, 0
ff =    0, 0, 0, 0
[[[Slab 1]]]
B =  0, 0, 1, 1
thetaB =  0, 0, 1, 1
chiB =  0, 0, 1, 1
vdopp =  1, 1, 0, 0
tau =  1, 1, 0, 0
vmac =  1, 1, 0, 0
[[[Slab 2]]]
B =  0, 0, 0, 0
thetaB =  0, 0, 0, 0
chiB =  0, 0, 0, 0
vdopp =  0, 0, 0, 0
tau =  0, 0, 0, 0
vmac =  0, 0, 0, 0
[[Weights]]
Stokes I =  1.0, 1.0, 1.0, 1.0
```

```
Stokes Q =  0.0, 0.0, 1.0, 1.0
Stokes U =  0.0, 0.0, 1.0, 1.0
Stokes V =  0.0, 0.0, 1.0, 1.0
```

4   Input files

HAZEL is controlled via four configuration files. All configuration files are fully commented, so that changing any parameter should be an easy task. In the following, we describe them step by step.

4.1   `config_inversion.dat`

This file can be considered as the main configuration file and it is the only one that has to have a fixed name. This file is used to indicate the names of the input files, the names of the output files, verbosity level and to decide whether HAZEL is to be applied to work in synthesis or inversion mode. Using the example included in the present version of HAZEL, we analyze one by one all the inputs.

```
# Input model file
'ATOMS/helium.mod'
```

Definition of the file with the atomic model. See §5 for an explanation of the file format.

```
# Initial parameters file
'init_parameters.dat'
```

Definition of the file with the initial parameters of the problem. The values of the parameters in this file are taken as initial values for the inversion or for the synthesis. See §4.2 for a detailed description of the file.

```
# Range of parameters for the DIRECT method
'direct_range.dat'
```

This file is used to define the lower and upper limits of the intervals inside which the DIRECT method searches for the minimum of the χ^2 function. See §4.3 for details.

```
# Output for the upper level rho^K_Q(J,J') in the vertical reference frame
'ATOMIC_POL/vertical_upper.rho'
```

```
# Output for the lower level rho^K_Q(J,J') in the vertical reference frame
'ATOMIC_POL/vertical_lower.rho'
```

```
# Output for the upper level rho^K_Q(J,J') in the mag. field reference frame
'ATOMIC_POL/magnetic_upper.rho'
```

```
# Output for the lower level rho^K_Q(J,J') in the mag. field reference frame
'ATOMIC_POL/magnetic_lower.rho'
```

The previous lines define the output files where the spherical tensor components of the density matrix are saved. Note that the code stores only the density matrix elements of the upper and lower level of the desired transition. The elements of the atomic density matrix depend on the chosen reference system, and the two most desired reference systems are the one in which the quantization axis is chosen along the solar local vertical direction and the one in which the quantization axis is chosen along the magnetic field vector.

```
# Output absorption/emission coefficients
'INVERTED/rtcoef.emer'
```

```
# Output absorption/emission coefficients neglecting atomic polarization
'INVERTED/rtcoef_noatompol.emer'
```

The emission coefficients $\epsilon_{I,Q,U,V}$, the absorption coefficients $\eta_{I,Q,U,V}$ and the anomalous dispersion coefficients $\rho_{Q,U,V}$ for each wavelength point are saved in these files. The first file includes the effects of atomic level polarization, while the second one neglects its influence.

```
# File with the observed profiles
'OBSERVATION/test.prof'
```

When using the code in the inversion mode, this file is the one used for the input of the observed Stokes profiles. The format of this file depends on which version of the code is used. For HAZEL, it is very simple. The first line indicates the number of wavelength points. Then, a table with nine columns gives the value of the wavelength shift with respect to the center of the multiplet, the Stokes vector at each wavelength normalized to the maximum intensity, and an estimation of the noise standard deviation at each wavelength normalized to the maximum intensity. See the example file contained in the HAZEL distribution for more details. Note that these lines have to be present in the input file even if HAZEL is used in synthesis mode.

When using P-HAZEL, the input file is more complicated and is described in §7.

```
# File with the inverted profiles
'test.inversion'
```

```
# File with the parameters from the inversion
'test.parameters'
```

The final Stokes profiles resulting from the synthesis or inversion options is saved in the file indicated in the first line. The format is the same as that explained for the file containing the observation. When HAZEL is run in inversion mode, the final inferred parameters of the model are saved in the file indicated in the second line. Again, for P-HAZEL the output files are described in §7.

```
# File that sets the parameters to invert
'invert_parameters.dat'
```

This file defines which parameters to invert in the inversion mode, together with the algorithm to be used in each cycle and the weight used for each Stokes parameter.

```
# Verbose mode (0-> no, 1-> yes)
0
```

Flag to connect or disconnect the verbose mode. For the inversion of Stokes profiles affected by atomic level polarization it is sometimes useful to turn the verbose mode on for analyzing the process of the code while calculating.

```
# Linear system solver (0-> LU, 1-> CG)
0
```

This flag is used to choose the algorithm that solves the linear system of statistical equilibrium equations. For relatively simple models, the LU decomposition does a very good job in terms of speed. If the number of unknowns (i.e., of $\rho_Q^K(J, J')$ elements) turns out to be of the order of or larger than 10^3, conjugate gradients (CG) methods are a much better option. We recommend to use the LU decomposition when possible and move to the CG solution only when necessary. The CG solution are based on routines developed by Dr. Mark K. Seager from Lawrence Livermore National Lab.

```
# Optically thin (0), slab no-MO (1), M-E (2), slab DELOPAR (3),
                      simplified slab (4), exact slab (5)
5
```

This flag is used to choose the level of approximation for the solution of the radiative transfer equation. The meaning of each option is explained below in §9.1.

```
# Synthesis mode -> 0 , Inversion mode -> 1
0
```

This flag controls the working mode of the code (synthesis or inversion).

4.2   init_parameters.dat

This important file establishes the parameters of the model, together with the definition of the scattering geometry. It includes also flags to turn on or discard different physical mechanisms. In the synthesis mode, the values in this file are used to carry out the synthesis. In the inversion mode, the values in this file are chosen as initial conditions for the inversion for those parameters that are left free. For those that are left fixed, the code uses the values defined in this file. We explain them step by step.

```
# Include stimulated emission (0-> no, 1-> yes)
1
```

This flag is used to take into account or discard the effect of stimulated emission in the emergent Stokes profiles. Although stimulated emission is negligible for most solar it can be of importance for very strong radiation fields. We recommend to use always 1 since the computational time is barely affected by this flag.

```
# Include magnetic field (0-> no, 1-> yes)
1
```

This flag is used to slightly reduce the computational work for the non-magnetic case because, if set to zero, the magnetic kernel [see Eq. (12)] is not calculated.

```
# Include depolarization rates (0-> no, 1-> yes)
0
```

```
# Value of delta if depol. rates are included (not used if prev. value = 0)
1.d14
```

In the present version of HAZEL it is possible to include the effect of depolarizing collisions only in the ground level of the atomic system. In case the effect of collisions is to be accounted for, set the first parameter to 1 and give the collisional rate in the next parameter in units of s^{-1}.

```
# Include Paschen-Back effect (0-> no, 1-> yes)
1
```

The effect of a magnetic field on the energy levels of the atomic system can be calculated under the approximation of the linear Zeeman effect or in the general case of the intermediate Paschen-Back effect. If this flag is set to 0, the approximation of the linear Zeeman effect is used and no perturbations between different J levels of a term are taken into account. If the flag is set to 1, the general theory of the Paschen-Back effect is used to calculate the wavelength positions and the strengths of the π and σ components. The difference in the computational work between both approaches is rather small.

```
# Number of slabs (1-> 1 slab, 2-> 2 slabs with same B,
3-> 2 slabs with different B, -2 -> 2 slabs with filling factor)
```

HAZEL can be used using one slab (option 1) of constant physical properties or two (options 2 and 3 and -2). The difference between options 2 and 3 is that option 2 considers both slabs to have exactly the same field while option 3 considers two different fields. As a consequence, the computing time is smaller in option 2. In both options, the second slab is placed in front of the first one, so that the boundary condition of the second slab is the emergent radiation from the first. In option -2, the radiation emerging from both slabs is added weighted with a filling factor, which is indicated below.

```
# Magnetic field strength [G], thetaB [degrees], chiB [degrees]
0.3d0 90.d0 90.d0
```

The magnetic field vector is defined here. The strength in G and the inclination and azimuth angles in degrees define the magnetic field vector. The angles are defined with respect to the vertical direction in the atmosphere, as shown in Fig. 3. Note that, if the azimuth of the field is set to 999, the random azimuth solution is obtained following the strategy explained in Appendix C of Belluzzi et al. (2007). If two slabs are used (setting option 3 or -2 above), put the two field vectors next to each one in the format $(B, \theta_B, \chi_B)_1 (B, \theta_B, \chi_B)_2$.

```
# Apparent height (if <0) or real height (if >0) of the atoms in arcsec
3.d0
```

The tensors J_0^0 and J_0^2 that quantify the mean intensity of the radiation field and its anisotropy are calculated assuming a standard solar center-to-limb variation (CLV) and taking into account geometrical effects. This parameter gives the height at which the slab of atoms is placed with respect to the surface of the Sun.

```
# Optical depth of the slab in the maximum of I (slab) or strength of the line (ME)
1.0d0
```

This quantity is the optical depth of the slab at the wavelength position of the maximum absorption or emission in Stokes I. For example, for the 10830 Å multiplet of He I, this is the position of the red blended component. If two slabs with option 2 or 3 are used, put the two optical depths together. If option -2 is used, then add the filling factor as a third number.

```
# Source function increase
1.d0
```

The source function of the slab will be multiplied by this number. This is a way to generate lines in emission even when the slab is seen on the solar disk. If two components (one after the other) are used, this number only modifies the source function of the second component. This allows us to simulate self-absorption in the code.

```
# Boundary Stokes parameters (I0,Q0,U0,V0)
4.098d-5 0.d0 0.d0 0.d0
```

Boundary conditions for the Stokes vector used in the solution of the radiative transfer equation. If the radiation field is the photospheric continuum, the IDL routine IDL_routines/solar_field.pro can be used to return an estimation.

```
# Transition where to compute the emergent Stokes profiles
1
```

From the transitions defined in the atomic model, the code calculates the emergent Stokes profiles for the chosen transition. For the moment, only one transition at a time is allowed. We plan to extend this to synthesize several lines.

```
# Include atomic level polarization? (0-> no, 1-> yes)
1
```

The synthesis or inversion options can be used taking into account or neglecting the presence of atomic level polarization. This flag controls it.

```
# Observation angle with respect to the local solar vertical theta,chi,gamma [degrees]
0.d0 0.d0 90.d0
```

The line-of-sight direction is defined using the angles described in Fig. 3. All angles are given in degrees.

```
# Wavelength axis: minimum, maximum and number of grid points
-3.d0 2.5d0 200
```

In case the code is run in synthesis mode, this line is used to set the lower and upper limits (in cm^{-1}) of the wavelength axis. The last parameter gives the number of wavelength points to be used. In the inversion mode, the wavelength axis is chosen automatically from the observation and these numbers are overridden.

```
# Line wavelength [A], Doppler velocity [km/s] and damping [a]
10829.0911d0    6.5d0    0.d0
```

This line is used to define the wavelength of the multiplet (wavelength of the $(L, S) \rightarrow (L', S')$ transition), the Doppler width of the line in km s^{-1} and the reduced damping constant. If two slabs (through options 3 or -2) are used, add the Doppler width of the second component next to the first one. Concerning the reduced damping constant, if its value is negative, it is computed using the natural damping and using the Doppler broadening. The absolute value of the input value is used then as an enhancement factor (so you should use -1 is you want to use the natural width).

```
# Macroscopic velocity [km/s] (>0 is a redshift)
0.d0
```

This defines the wavelength shift produced by the presence of a bulk motion of the plasma. Note that positive velocities imply redshifts. If two components (options 2, 3 or -2) are used, put the two bulk velocities.

```
# Include magneto-optical effects in the RT
1
```

It is possible to include (1) or neglect (0) the influence of the anomalous dispersion coefficients $\rho_{Q,U,V}$ in the calculation of the emergent Stokes profiles.

```
# Include stimulated emission in the RT
1
```

This flag controls whether we include (1) or neglect (0) the influence of the stimulated emission in the calculation of the emergent Stokes profiles.

4.3 `direct_range.dat`

The DIRECT global optimization method is used to give a first estimation of the parameters from which the Levenberg-Marquardt method is applied to locate the minimum of the χ^2 surface. The behavior of the DIRECT method is controlled with this file, in which we must specify the upper and lower limits of the model parameters, together with details about the stopping criterion. In the following, we describe all the options in detail.

```
# Output file
'direct.location'
```

The DIRECT method tries to evaluate the merit function χ^2 as few times as possible. The code saves in this file the values of the parameters at which the algorithm has carried out the evaluation of the merit function. This can be useful for analyzing the presence of ambiguities. In this case, the method will clearly mark the position of the possible solutions by evaluating the merit function more times in the surroundings of the compatible solutions. Note that this lines are absent on the P-Hazel configuration file.

```
# Maximum number of function evaluations (<0 -> don't use this criteria)
-1
```

```
# Reduction in the volume (<0 -> don't use this criteria, typically 0.01)
0.001
```

The previous two lines are used to indicate the stopping criterion for the DIRECT method. An early stop will probably give a first estimation of the solution that is far from the final result. Letting the code run for many iterations may degrade too much the computing time because of the poor local convergence properties of the DIRECT scheme. The first option permits the user to stop after a fixed number of evaluations of the merit function. The second option permits the user to stop when the ratio between the hypervolume where the global minimum is located and the original hypervolume is smaller than the given threshold. We have verified that 0.001 gives very good results. Setting one of the two parameters to values < 0 will disconnect it.

```
# Magnetic field (0-Bmax)
800.d0  1100.d0
```

```
# thetab  (0 .. 180)
30.d0  180.d0
```

```
# chib (0 .. 180)
-180.d0  0.d0
```

```
# vdopp (0 .. 20)
2.d0  7.d0
```

```
# dtau (0 .. 5)
0.d0   1.d0


# delta_collision (0 .. 18)
0.d0   18.d0


# vmacro (-10 .. 10)
-10.d0   10.d0


# damping (0 .. 4)
0.d0   4.d0


# beta (0 .. 10)
0.d0   1.d0


# height (0 .. 100)
0.d0   100.d0


# dtau2 (0 .. 5)
0.d0   2.d0


# vmacro2 (-10 .. 10)
25.d0   35.d0


# Magnetic field 2 (0-Bmax)
800.d0   1100.d0


# thetab 2 (0 .. 180)
30.d0   180.d0


# chib 2 (0 .. 180)
-180.d0   0.d0


# vdopp 2 (0 .. 20)
2.d0   12.d0
```

The previous lines define the space of parameters where the DIRECT method will look for the global minimum.

4.4   invert_parameters.dat

This file is used to set the behavior of the inversion mode: the structure of the inversion cycle, setting the free and the fixed parameters.

```
# Maximum number of iterations
20
```

This parameter sets the maximum number of Levenberg-Marquardt (LM) iterations to be carried out in each cycle. Sometimes the LM scheme stops before reaching the maximum number of iterations because the relative change in the parameters from one iteration to the next is below 10^{-4}.

```
# Number of cycles
2
```

The optimal iteration scheme is composed of combinations of cycles. In the first cycle, the DIRECT method is used to give a first estimation of the solution. In the second cycle, the LM method is used to refine the solution until arriving to the final one. This parameter sets the number of cycles used.

```
# Invert the magnetic field strength
1 1 1 1
```

```
# Invert the magnetic field inclination
1 1 1 1
```

```
# Invert the magnetic field azimuth
1 1 0 0
```

```
# Invert the Doppler width
0 0 0 0
```

```
# Invert the optical depth or strength of the line
0 0 0 0
```

```
# Invert the D^2 of the lower level
0 0 0 0
```

```
# Invert the macroscopic velocity
0 0 0 0
```

```
# Invert the damping
0 0 0 0
```

```
# Invert the source function gradient
0 0 0 0
```

```
# Invert the height of the He atoms
0 0 0 0
```

```
# Invert the optical depth or strength of the line of component 2
0 0 0 0
```

```
# Invert the macroscopic velocity of component 2
0 0 0 0
```

```
# Invert the magnetic field strength of component 2
0 0 1 1
```

```
# Invert the magnetic field inclination of component 2
0 0 1 1
```

```
# Invert the magnetic field azimuth of component 2
0 0 1 1
```

```
# Invert the Doppler width of component 2
0 0 0 0
```

Depending on the number of cycles, the previous lines define whether a parameter is inverted (setting a 1 in the corresponding cycle) or kept fixed to the value given in the `init_parameters.dat` file (setting a 0 in the corresponding cycle). The number of 0s/1s in each line has to be larger or equal to the number of cycles.

```
# Weights for Stokes I in each cycle
1.d0 1.d0 1.d0 1.d0
```

```
# Weights for Stokes Q in each cycle
1.d0 1.d0 1.d0 1.d0
```

```
# Weights for Stokes U in each cycle
1.d0 1.d0 1.d0 1.d0
```

```
# Weights for Stokes V in each cycle
1.d0 1.d0 1.d0 1.d0
```

Since the inversion is based on the gradient descent minimization of the χ^2 merit function and not on sampling methods, it is important to modify sometimes the weight of each Stokes vector in order to increase the sensitivity of the χ^2-function to some model parameters. The code allows to change the relative weight of each Stokes vector in each cycle.

```
# Inversion modes (1-> LM, 2-> DIRECT, 3-> PIKAIA)
2 1 2 1
```

The optimization method used in each cycle is set in this line. Note that the scheme DIRECT+LM has been empirically proved to be quite optimal. The possibility to use genetic optimization based on the Pikaia algorithm is still in a preliminary phase. However, the large number of function evaluations that any genetic algorithm needs makes it difficult to beat the DIRECT+LM combination.

5 Atomic models

Atomic models have to be defined in HAZEL in order to carry out a calculation. This section describes the model atom file in detail by using the example `helium.mod` that is included in the present version of HAZEL.

```
2
5
```

The previous two numbers define the general properties of the atom. The first line of the file is equal to $2S$, where S is the value of the spin of the terms. In the example, $S = 1$. At present, the code does not treat transitions between terms of different multiplicity which are, otherwise, of reduced importance due to their small transition probability. The second line contains the number of terms included in the model atom. This example represents the triplet system of He I with the lowest five terms, $2s^3S$, $3s^3S$, $2p^3P$, $3p^3P$ and $3d^3D$

```
1          0
              0.00
2          2
              0.00
             -0.987913
             -1.064340
3          0
              0.00
4          2
              0.00
             -0.270647
             -0.292616
5          4
              0.00
             -0.044187
             -0.046722
```

The previous lines define the term levels included in the model. The information for each term consist of a line with an index $(0,1,2,\ldots)$ that is used just to label each term and the value of $2L$, where L is the value of the electronic orbital angular momentum. Then, for each term, we must supply a list containing the energy separation in cm^{-1} between each J-level and the level with the smallest absolute value of J. In case only one value of J is possible in the term, just put 0 in the energy difference.

```
 4
1     1     2     1.022d7     10829.0911     1.0000000     1.0000000     0.0000000
2     1     4     9.478d6     3888.6046      0.2000000     1.0000000     0.0000000
3     2     3     2.780d7     7065.7085      1.0000000     1.0000000     0.0000000
4     2     5     7.060d7     5875.9663      1.0000000     1.0000000     0.0000000
```
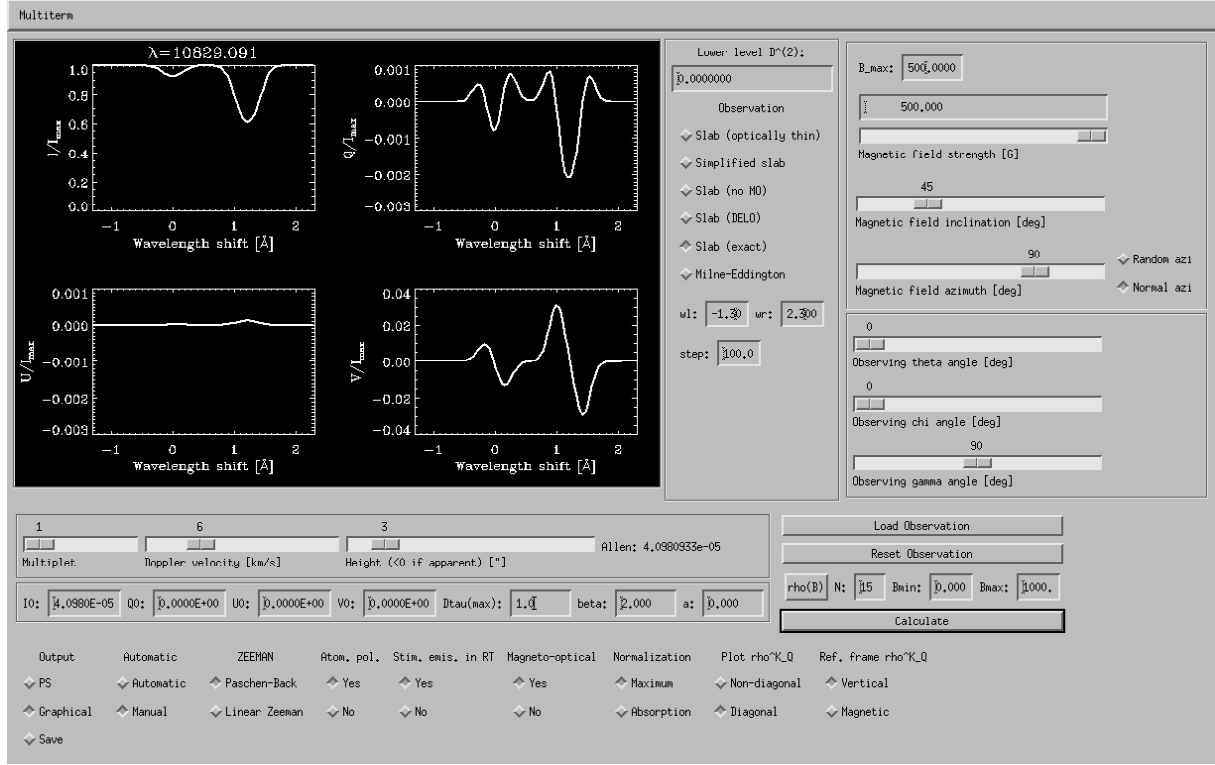
Figure 1: Screen dump of the graphical front-end used for the synthesis.

Finally, the list of transitions has to be supplied. The first number indicates the number of radiative transitions included in the model. Then, the list contains the following numbers for each transition: index number, index of lower level, index of upper level, Einstein coefficient for spontaneous emission A_{ul} of the transition, modification factor $f(\bar{n})$, modification factor $f(w)$ and value of J_0^1/J_0^0. The modification factors $f(\bar{n})$ and $f(w)$ are multiplied by the mean number of photons per mode $\bar{n}$ and the anisotropy factor w, respectively. Since HAZEL uses the value of $\bar{n}$ and w calculated from the tabulated solar CLV and taking into account geometrical effects, these factors can be used to analyze the behavior of the emergent Stokes profiles when, for some reason, the anisotropy or the intensity of the radiation field is increased or decreased by an arbitrary factor. Finally, if the radiation illuminating the atoms has non-zero net circular polarization, it is possible to include its effect in the statistical equilibrium equations by giving the value of J_0^1/J_0^0.

6   Graphical front-ends

Although the code can be run in command line by modifying by hand the input files, HAZEL contains also two user friendly front-ends (GUI) for the simple execution and analysis of the results. Note that the directory IDL_routines has to be in your IDL path.

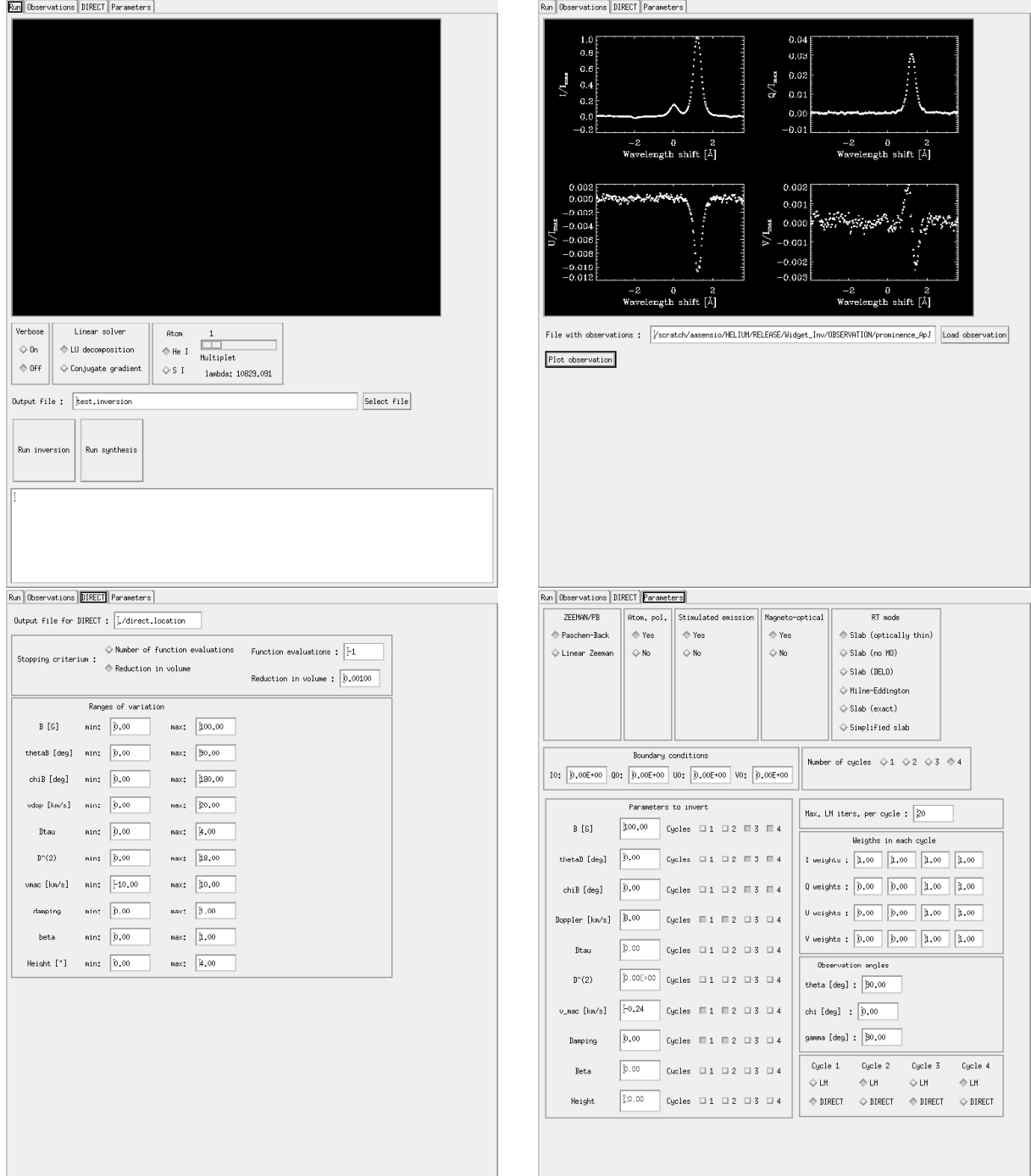Figure 2: Screen dump of the graphical front-end used for the inversion.

6.1 Synthesis

It is placed in the directory `Widget_Synth` and it is invoked with the following commands:

```
IDL> .r hazel
IDL> hazel
```

Figure 1 shows the GUI for the synthesis mode. All the parameters explained in the previous sections (fundamentally those in §4.2) are present in the GUI. All the parameters are very simple to modify (when changing numerical values in the GUI, always remember to press `Return` to activate the change) and clicking on **Calculate**, the window is updated with the new Stokes profiles. The GUI also shows the value of the solar radiation field when the inclination of the line-of-sight and the wavelength of the multiplet is changed. The value (which can be introduced in the value of I_0 as a boundary condition) is given next to the height of the slab and indicated with the label "Allen". In case of crashes, the GUI can be restarted with the following command:

```
IDL> .r hazel
IDL> hazel, /reset
```

6.2   Inversion

It is placed in the directory `Widget_Inv` and it is invoked with the following commands:

```
IDL> .r hazel_inv
IDL> hazel_inv
```

Again, in case of crashes, the GUI can be restarted with the following command:

```
IDL> .r hazel_inv
IDL> hazel_inv, /reset
```

The GUI for the inversion is more complex because of the large amount of parameters that have to be changed. For this reason, the GUI is composed of 4 pages, as indicated in Fig. 2.

The first page is used to select the output file, together with the atomic system and multiplet to be used. Finally, the button **Run inversion** will call Hazel and update the state of the best model in the plot window.

The second page is used simply to load the file with the observed Stokes profile. A button is also available to plot the observed data.

The third page controls the behavior of the DIRECT algorithm. It is essentially a graphical representation of the `direct_range.dat` file.

Finally, the fourth page controls the behavior of the cycles, the value of the fixed parameters, the weights for each Stokes parameter and the level of physical realism introduced in the simulation.

7   P-Hazel input/output files

Both input and output files for P-Hazel are NetCDF files.

7.1 Input files

The input file constains the observations and information about the observing position and boundary condition. The file consists of the following variables:

- lambda: vector of size *nlambda* containing the wavelength axis with respect to the center of the multiplet.

- map: array of size *(npixel,8,nlambda)* containing the Stokes vector (I, Q, U, V) and the associated standard deviation of the noise $(\sigma_I, \sigma_Q, \sigma_U, \sigma_V)$.

- boundary: array of size *(npixel,4)* containing the boundary condition for every inverted pixel.

- height: vector of size *npixel* which contains the height of the slabs for every pixel.

- obs_theta: vector of size *npixel* which contains the observing angle θ for every pixel.

- obs_gamma: vector of size *npixel* which contains the observing angle γ that defines the positive reference for Stokes Q for every pixel.

- mask: array of size *nx,ny* which tells whether this pixel will be inverted.

- pars: array of size *npixel,npars* which contains the initial value for the model parameters. These will be used to reinvert some pixels or, for instance, to refine the ambiguous solutions.

The routine `gen_netcdf.pro` on the directory `IDL_routines` shows a function that generates such a file by passing all the variables as parameters. The order of pars is the following, depending on the number of slabs:

- 1-component (vector of size 8): B, θ_B, χ_B, τ, v_{dop}, a, v_{mac}, β

- 2-component 1+1 with same field (vector of size 10): B, θ_B, χ_B, τ_1, τ_2, v_{dop}, a, v_{mac1}, v_{mac2}, β

- 2-component 1+1 with different field (vector of size 14): B_1, θ_{B1}, χ_{B1}, B_2, θ_{B2}, χ_{B2}, τ_1, τ_2, v_{dop}, v_{dop2}, a, v_{mac1}, v_{mac2}, β

- 2-component 2 with different field with filling factor (vector of size 14): B_1, θ_{B1}, χ_{B1}, B_2, θ_{B2}, χ_{B2}, τ_1, τ_2, v_{dop}, v_{dop2}, a, v_{mac1}, v_{mac2}, ff

7.2 Output files

The results of the inversion are saved on two files defined on the `config_inversion.dat` configuration file. The file with the inverted profiles contains the following variables:

- lambda: vector of size *nlambda* containing the wavelength axis with respect to the center of the multiplet.

- map: array of size *(npixel,4,nlambda)* containing the synthetic Stokes vector (I, Q, U, V) for every pixel.

The file with the inverted parameters contains the following variable:

- map: array of size *(npixel,ncolumns)* containing the parameters of the inversion.

The number of columns depends on the selected model:

- One-slab: nine columns with the vector $(B, \theta_B, \chi_B, h, \tau, v_{\text{th}}, a, v_{\text{mac}}, \beta)$.

- Two-slab with same magnetic field: eleven columns with the vector $(B, \theta_B, \chi_B, h, [\tau]_1, [\tau]_2, v_{\text{th}}, a, [v_{\text{mac}}]_1, [v_{\text{mac}}]_2, \beta)$.

- Two-slab with different magnetic field: fifteen columns with the vector $([B]_1, [\theta_B]_1, [\chi_B]_1, [B]_2, [\theta_B]_2, [\chi_B]_2, h, [\tau]_1, [\tau]_2, [v_{\text{th}}]_1, [v_{\text{th}}]_2, a, [v_{\text{mac}}]_1, [v_{\text{mac}}]_2, \beta)$.

The file `read_results.pro` on the `RunMPI` directory shows how to read the files from IDL.

7.3 Ambiguities

You have to remember that the results of Hazel are potentially affected by ambiguities and you have to take them into account. There is an utility written in IDL that, given an inverted map, obtains all the other solutions which are ambiguous in the saturation regime. This can be called, including the appropriate paths and discarding the final `.nc` extension, by:

```
IDL> disamb, 'file_with_inversions', 'file_with_observations', angleObs
```

where `angleObs` is the observation angle θ (so that it is 90° for an observation exactly at the limb. This program can be called with the additional `/gen_files_inversion`, which then generates a set of observations, configuration files and a file to run P-Hazel. This is useful in case the line is not in the saturation regime. In this case, the ambiguous solutions that are found by the code are not strictly valid and one should refine them with a final LM cycle in which B, θ_B and χ_B are left free. The solution to the ambiguities in the saturation regime is shown in Section 11.

8 Calling Hazel from Python

We have developed a wrapper to allow the user to call the synthesis routines of Hazel in Python. To do so, just enter into the directory `SourcePy` and type

```
python setup.py build_ext --inplace
```

and a library `pyhazel.so` will be generated (and also copied to the directory `RunPy`. In this very same directory you can see the `test.py` file that shows how to call the code to wrapper.

9 Basic Equations

We consider a constant-property slab of atoms, located at a height h above the visible solar "surface", in the presence of a deterministic magnetic field of arbitrary strength B, inclination θ_B and azimuth χ_B (see Fig. 1). The slab's optical thickness at the wavelength and line of sight under consideration is τ. We assume that all the atoms inside this slab are illuminated from below by the photospheric solar continuum radiation field, whose center-to-limb variation has been tabulated by Pierce (2000). The ensuing anisotropic radiation pumping produces population imbalances and quantum coherences between pairs of magnetic sublevels, even among those pertaining to the different J-levels of the adopted atomic model. This atomic level polarization and the Zeeman-induced wavelength shifts between the π ($\Delta M = M_u - M_l = 0$), σ_{blue} ($\Delta M = +1$) and σ_{red} ($\Delta M = -1$) transitions produce polarization in the emergent spectral line radiation.

In order to facilitate the understanding of the code, in the following we summarize the basic equations which allow us to calculate the spectral line polarization taking rigorously into account the joint action of atomic level polarization and the Hanle and Zeeman effects. To this end, we have applied the quantum theory of spectral line polarization, which is described in great detail in the monograph by Landi Degl'Innocenti & Landolfi (2004). We have also applied several methods of solution of the Stokes-vector transfer equation, some of which can be considered as particular cases of the two general methods explained in §6 of Trujillo Bueno (2003).

9.1 The radiative transfer approach

The emergent Stokes vector $\mathbf{I}(\nu, \mathbf{\Omega}) = (I, Q, U, V)^{\dagger}$ (with $\dagger$=transpose, ν the frequency and $\mathbf{\Omega}$ the unit vector indicating the direction of propagation of the ray) is obtained by solving the radiative transfer equation

$$\frac{d}{ds}\mathbf{I}(\nu, \mathbf{\Omega}) = \boldsymbol{\epsilon}(\nu, \mathbf{\Omega}) - \mathbf{K}(\nu, \mathbf{\Omega})\mathbf{I}(\nu, \mathbf{\Omega}), \tag{1}$$

where s is the geometrical distance along the ray under consideration, $\boldsymbol{\epsilon}(\nu, \mathbf{\Omega}) = (\epsilon_I, \epsilon_Q, \epsilon_U, \epsilon_V)^{\dagger}$ is the emission vector and

$$\mathbf{K} = \begin{pmatrix} \eta_I & \eta_Q & \eta_U & \eta_V \\ \eta_Q & \eta_I & \rho_V & -\rho_U \\ \eta_U & -\rho_V & \eta_I & \rho_Q \\ \eta_V & \rho_U & -\rho_Q & \eta_I \end{pmatrix} \tag{2}$$

is the propagation matrix. Alternatively, introducing the optical distance along the ray, $\mathrm{d}\tau = -\eta_I \mathrm{d}s$, one can write the Stokes-vector transfer Eq. (1) in the following two ways:

- The first one, whose formal solution requires the use of the evolution operator introduced by Landi Deglinnocenti & Landi Deglinnocenti (1985), is

$$\frac{d}{d\tau}\mathbf{I} = \mathbf{K}^*\mathbf{I} - \mathbf{S}, \tag{3}$$

  where $\mathbf{K}^* = \mathbf{K}/\eta_I$ and $\mathbf{S} = \boldsymbol{\epsilon}/\eta_I$. The formal solution of this equation can be seen in eq. (23) of Trujillo Bueno (2003).
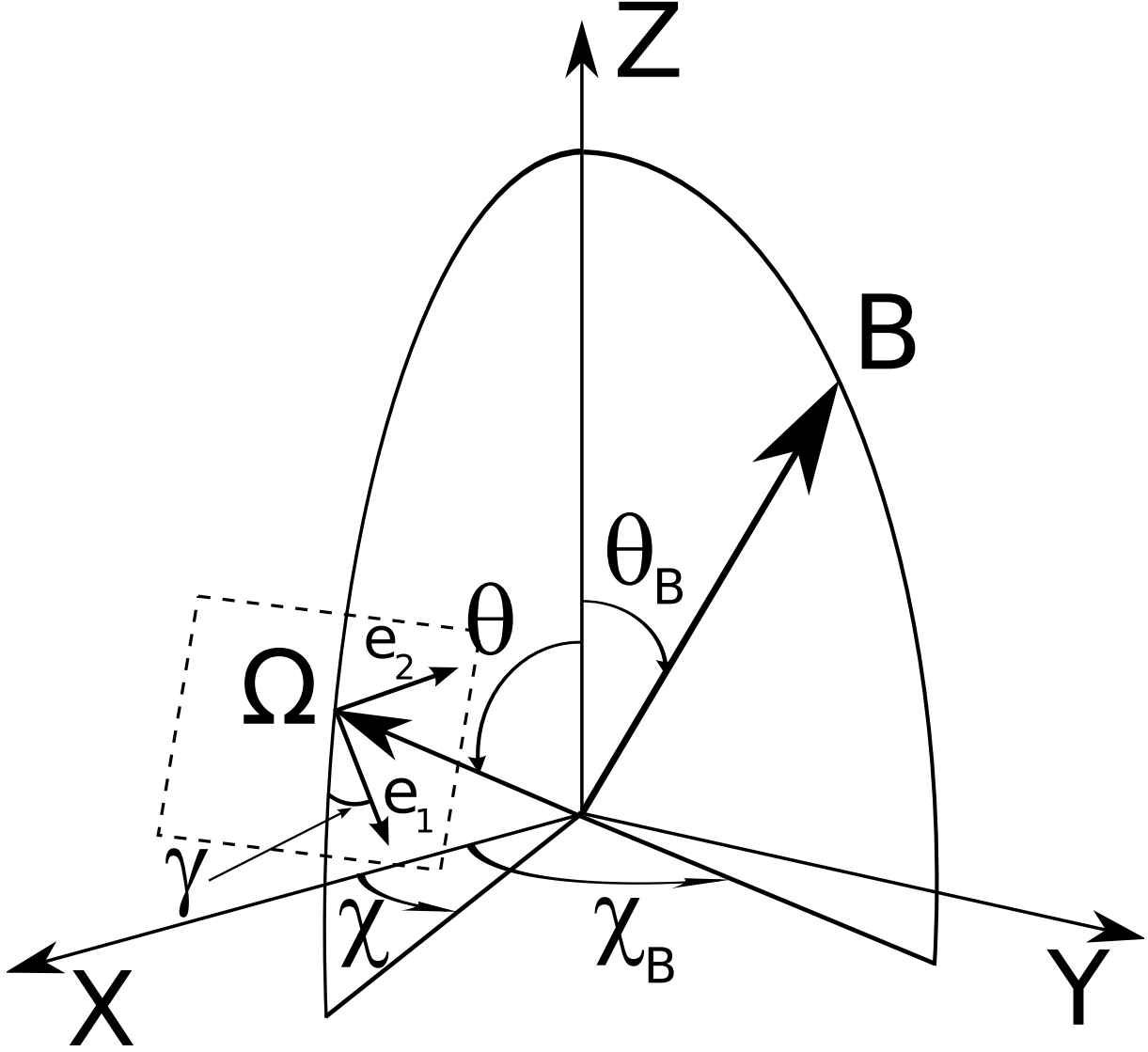
Figure 3: The geometry for the scattering event. The Z-axis is placed along the vertical to the solar atmosphere. The magnetic field vector, $\mathbf{B}$, is characterized by its modulus B, the inclination angle θ_B and the azimuth χ_B. The line-of-sight, indicated by the unit vector $\mathbf{\Omega}$, is characterized by the two angles θ and χ. The reference direction for Stokes Q is defined by the vector $\mathbf{e}_1$ on the plane perpendicular to the line-of-sight. This vector makes an angle γ with respect to the plane formed by the vertical and the line-of-sight. In the figures showing examples of the emergent Stokes profiles, our choice for the positive reference direction for Stokes Q is $\gamma = 90°$, unless otherwise stated. For off-limb observations, we have $\theta = 90°$, while for observations on the solar disk, we have $\theta < 90°$. Note also that χ is generally taken to be $0°$.

- The second one, whose formal solution does not require the use of the above-mentioned evolution operator is (e.g., Rees et al., 1989)

$$\frac{d}{d\tau}\mathbf{I} = \mathbf{I} - \mathbf{S}_{\text{eff}}, \tag{4}$$

where the effective source-function vector $\mathbf{S}_{\text{eff}} = \mathbf{S} - \mathbf{K'I}$, being $\mathbf{K'} = \mathbf{K^*} - \mathbf{1}$ (with $\mathbf{1}$ the unit matrix). The formal solution of this equation can be seen in eq. (26) of Trujillo Bueno (2003).

Once the coefficients ϵ_I and ϵ_X (with $X = Q, U, V$) of the emission vector and the coefficients η_I, η_X, and ρ_X of the 4×4 propagation matrix are known at each point within the medium it is possible to solve formally Eq. (3) or Eq. (4) for obtaining the emergent Stokes profiles for any desired line of sight. Our computer program considers the following levels of sophistication for the solution of the radiative transfer equation:

- *Numerical Solutions.* The most general case, where the properties of the slab vary along the ray path, has to be solved numerically. To this end, two efficient and accurate methods of solution of the Stokes-vector transfer equation are those proposed by Trujillo Bueno (2003) (see his eqs. (24) and (27), respectively). The starting points for the development of these two numerical methods were Eq. (3) and Eq. (4), respectively. Both methods can be considered as generalizations, to the Stokes-vector transfer case, of the well-known short characteristics method for the solution of the standard (scalar) transfer equation.

- *Exact analytical solution of the problem of a constant-property slab including the magneto-optical terms of the propagation matrix.* For the general case of a constant-property slab of arbitrary optical thickness we actually have the following analytical solution, which can be easily obtained as a particular case of eq. (24) of Trujillo Bueno (2003):

$$\mathbf{I} = e^{-\mathbf{K^*}\tau}\,\mathbf{I}_{\text{sun}} + [\mathbf{K^*}]^{-1}\left(\mathbf{1} - e^{-\mathbf{K^*}\tau}\right)\mathbf{S}, \tag{5}$$

where $\mathbf{I}_{\text{sun}}$ is the Stokes vector that illuminates the slab's boundary that is most distant from the observer. We point out that the exponential of the propagation matrix $\mathbf{K^*}$ has an analytical expression similar to eq. (8.23) in Landi Degl'Innocenti & Landolfi (2004).

- *Approximate analytical solution of the problem of a constant-property slab including the magneto-optical terms of the propagation matrix.* An approximate analytical solution to the constant-property slab problem can be easily obtained as a particular case of eq. (27) of Trujillo Bueno (2003):

$$\mathbf{I} = [\mathbf{1} + \Psi_0\mathbf{K'}]^{-1}\left[\left(e^{-\tau}\mathbf{1} - \Psi_M\mathbf{K'}\right)\mathbf{I}_{\text{sun}} + (\Psi_M + \Psi_0)\mathbf{S}\right], \tag{6}$$

28

where the coefficients Ψ_M and Ψ_0 depend only on the optical thickness of the slab at the frequency and line-of-sight under consideration, since their expressions are:

$$\begin{aligned}
\Psi_M &= \frac{1 - e^{-\tau}}{\tau} - e^{-\tau}, \\
\Psi_0 &= 1 - \frac{1 - e^{-\tau}}{\tau}.
\end{aligned} \tag{7}$$

Note that Eq. (6) for the emergent Stokes vector is the one used by Trujillo Bueno & Asensio Ramos (2007) for investigating the impact of atomic level polarization on the Stokes profiles of the He I 10830 Å multiplet. We point out that, strictly speaking, it can be considered only as the exact analytical solution of the optically-thin constant-property slab problem[2]. The reason why Eq. (6) is, in general, an approximate expression for calculating the emergent Stokes vector is because its derivation assumes that the Stokes vector within the slab varies linearly with the optical distance. However, it provides a fairly good approximation to the emergent Stokes profiles (at least for all the problems we have investigated in this paper). Moreover, the results of fig. 2 of Trujillo Bueno & Asensio Ramos (2007) remain also virtually the same when using instead the exact Eq. (5), which from a computational viewpoint is significantly less efficient than the approximate Eq. (6).

- *Exact analytical solution of the problem of a constant-property slab when neglecting the second-order terms of the Stokes-vector transfer equation.* Simplified expressions for the emergent Stokes vector can be obtained when $\epsilon_I \gg \epsilon_X$ and $\eta_I \gg (\eta_X, \rho_X)$, which justifies to neglect the second-order terms of Eq. (1). The resulting approximate formulae for the emergent Stokes parameters are given by eqs. (9) and (10) of Trujillo Bueno & Asensio Ramos (2007), which are identical to those used by Trujillo Bueno et al. (2005) for modeling the Stokes profiles observed in solar chromospheric spicules. We point out that there is a typing error in the sentence that introduces such eqs. (9) and (10) in Trujillo Bueno & Asensio Ramos (2007), since they are obtained only when the above-mentioned second-order terms are neglected in Eq. (1), although it is true that there are no magneto-optical terms in the resulting equations.

- *Optically thin limit.* Finally, the most simple solution is obtained when taking the optically thin limit ($\tau \ll 1$) in the equations reported in the previous point, which lead to the equations (11) and (12) of Trujillo Bueno & Asensio Ramos (2007). Note that if $\mathbf{I}_{\mathrm{sun}} = 0$ (i.e., $I_0 = X_0 = 0$), then such optically thin equations imply that $X/I \approx \epsilon_X/\epsilon_I$.

The coefficients of the emission vector and of the propagation matrix depend on the multipolar components, $\rho_Q^K(J, J')$, of the atomic density matrix. Let us recall now the meaning of these physical quantities and how to calculate them in the presence of an arbitrary magnetic field under given illumination conditions.

---

[2]More precisely, when the optical thickness of the slab is small in comparison with the eigenvalues of the matrix $\mathbf{K}'$.

9.2 The multipolar components of the atomic density matrix

We quantify the atomic polarization of the atomic levels using the multipolar components of the atomic density matrix. We assume that the atom can be correctly described under the framework of the L-S coupling (e.g., Condon & Shortley, 1935). The different J-levels are grouped in terms with well defined values of the electronic angular momentum L and the spin S. We neglect the influence of hyperfine structure and assume that the energy separation between the J-levels pertaining to each term is very small in comparison with the energy difference between different terms. Therefore, we allow for coherences between different J-levels pertaining to the same term but not between the J-levels pertaining to different terms. As a result, we can represent the atom under the formalism of the multi-term atom discussed by Landi Degl'Innocenti & Landolfi (2004).

In the absence of magnetic fields the energy eigenvectors can be written using Dirac's notation as $|\beta LSJM\rangle$, where β indicates a set of inner quantum numbers specifying the electronic configuration. In general, if a magnetic field of arbitrary strength is present, the vectors $|\beta LSJM\rangle$ are no longer eigenfunctions of the total Hamiltonian and J is no longer a good quantum number. In this case, the eigenfunctions of the full Hamiltonian can be written as the following linear combination:

$$|\beta LSjM\rangle = \sum_J C_J^j(\beta LS, M)|\beta LSJM\rangle, \tag{8}$$

where j is a pseudo-quantum number which is used for labeling the energy eigenstates belonging to the subspace corresponding to assigned values of the quantum numbers β, L, S, and M, and where the coefficients C_J^j can be chosen to be real.

In the presence of a magnetic field sufficiently weak so that the magnetic energy is much smaller than the energy intervals between the J-levels, the energy eigenvectors are still of the form $|\beta LSJM\rangle$ ($C_J^j(\beta LS, M) \approx \delta_{Jj}$), and the splitting of the magnetic sublevels pertaining to each J-level is linear with the magnetic field strength. For stronger magnetic fields, we enter the incomplete Paschen-Back effect regime in which the energy eigenvectors are of the general form given by Eq. (8), and the splitting among the various M-sublevels is no longer linear with the magnetic strength. If the magnetic field strength is further increased we eventually reach the so-called complete Paschen-Back effect regime, where the energy eigenvectors are of the form $|LSM_LM_S\rangle$ and each L-S term splits into a number of components, each of which corresponding to particular values of $(M_L + 2M_S)$.

Within the framework of the multi-term atom model the atomic polarization of the energy levels is described with the aid of the density matrix elements

$$\rho^{\beta LS}(jM, j'M') = \langle \beta LSjM|\rho|\beta LSj'M'\rangle, \tag{9}$$

where ρ is the atomic density matrix operator. Using the expression of the eigenfunctions of the total Hamiltonian given by Eq. (8), the density matrix elements can be rewritten as:

$$\rho^{\beta LS}(jM, j'M') = \sum_{JJ'} C_J^j(\beta LS, M)C_{J'}^{j'}(\beta LS, M')\rho^{\beta LS}(JM, J'M'), \tag{10}$$

where $\rho^{\beta LS}(JM, J'M')$ are the density matrix elements on the basis of the eigenvectors $|\beta LSJM\rangle$.

Following Landi Degl'Innocenti & Landolfi (2004), it is helpful to use the spherical statistical tensor representation, which is related to the previous one by the following linear combination:

$$
\begin{aligned}
{}^{\beta LS}\rho_Q^K(J,J') \;=\; & \sum_{jj'MM'} C_J^j(\beta LS, M) C_{J'}^{j'}(\beta LS, M') \\
& \times \; (-1)^{J-M}\sqrt{2K+1} \begin{pmatrix} J & J' & K \\ M & -M' & -Q \end{pmatrix} \rho^{\beta LS}(jM, j'M'), \quad (11)
\end{aligned}
$$

where the 3-j symbol is defined as indicated by any suitable textbook on Racah algebra.

9.3 Statistical equilibrium equations

In order to obtain the ${}^{\beta LS}\rho_Q^K(J,J')$ elements we have to solve the statistical equilibrium equations. These equations, written in a reference system in which the quantization axis (Z) is directed along the magnetic field vector and neglecting the influence of collisions, can be written as (Landi Degl'Innocenti & Landolfi, 2004):

$$
\begin{aligned}
\frac{d}{dt}{}^{\beta LS}\rho_Q^K(J,J') \;=\; & -2\pi i \sum_{K'Q'}\sum_{J''J'''} N_{\beta LS}(KQJJ', K'Q'J''J''') {}^{\beta LS}\rho_{Q'}^{K'}(J'', J''') \\
& + \sum_{\beta_\ell L_\ell K_\ell Q_\ell J_\ell J'_\ell} {}^{\beta_\ell L_\ell S}\rho_{Q_\ell}^{K_\ell}(J_\ell, J'_\ell)\mathbb{T}_A(\beta LSKQJJ', \beta_\ell L_\ell SK_\ell Q_\ell J_\ell J'_\ell) \\
& + \sum_{\beta_u L_u K_u Q_u J_u J'_u} {}^{\beta_u L_u S}\rho_{Q_u}^{K_u}(J_u, J'_u)\Big[\mathbb{T}_E(\beta LSKQJJ', \beta_u L_u SK_u Q_u J_u J'_u) \\
& \qquad\qquad\qquad + \mathbb{T}_S(\beta LSKQJJ', \beta_u L_u SK_u Q_u J_u J'_u)\Big] \\
& - \sum_{K'Q'J''J'''} {}^{\beta LS}\rho_{Q'}^{K'}(J'', J''')\Big[\mathbb{R}_A(\beta LSKQJJ'K'Q'J''J''') \\
& + \mathbb{R}_E(\beta LSKQJJ'K'Q'J''J''') + \mathbb{R}_S(\beta LSKQJJ'K'Q'J''J''')\Big]. \quad (12)
\end{aligned}
$$

The first term in the right hand side of Eq. (12) takes into account the influence of the magnetic field on the atomic level polarization. This term has its simplest expression in the chosen magnetic field reference frame (see eq. 7.41 of Landi Degl'Innocenti & Landolfi, 2004). In any other reference system, a more complicated expression arises. The second, third and fourth terms account, respectively, for coherence transfer due to absorption from lower levels ($\mathbb{T}_A$), spontaneous emission from upper levels ($\mathbb{T}_E$) and stimulated emission from upper levels ($\mathbb{T}_S$). The remaining terms account for the relaxation of coherences due to absorption to upper levels ($\mathbb{R}_A$), spontaneous emission to lower levels ($\mathbb{R}_E$) and stimulated emission to lower levels ($\mathbb{R}_S$), respectively.

The stimulated emission and absorption transfer and relaxation rates depend explicitly on the radiation field properties (see eqs. 7.45 and 7.46 of Landi Degl'Innocenti & Landolfi, 2004). The symmetry properties of the radiation field are accounted for by the spherical components of the radiation field tensor:

$$J_Q^K(\nu) = \oint \frac{d\Omega}{4\pi} \sum_{i=0}^{3} \mathcal{T}_Q^K(i, \mathbf{\Omega}) S_i(\nu, \mathbf{\Omega}). \tag{13}$$

The quantities $\mathcal{T}_Q^K(i, \mathbf{\Omega})$ are spherical tensors that depend on the reference frame and on the ray direction $\mathbf{\Omega}$. They are given by

$$\mathcal{T}_Q^K(i, \mathbf{\Omega}) = \sum_P t_P^K(i) \mathcal{D}_{PQ}^K(R'), \tag{14}$$

where R' is the rotation that carries the reference system defined by the line-of-sight $\mathbf{\Omega}$ and by the polarization unit vectors $\mathbf{e}_1$ and $\mathbf{e}_2$ into the reference system of the magnetic field, while $\mathcal{D}_{PQ}^K(R')$ is the usual rotation matrix (e.g., Edmonds, 1960). Table 5.6 in Landi Degl'Innocenti & Landolfi (2004) gives the $\mathcal{T}_Q^K(i, \mathbf{\Omega})$ values for each Stokes parameter S_i (with $S_0 = I$, $S_1 = Q$, $S_2 = U$ and $S_3 = V$).

9.4 Emission and absorption coefficients

Once the multipolar components $^{\beta LS}\rho_Q^K(J, J')$ are known, the coefficients ϵ_I and ϵ_X (with $X = Q, U, V$) of the emission vector and the coefficients η_I, η_X, and ρ_X of the propagation matrix for a given transition between an upper term $(\beta L_u S)$ and an lower term $(\beta L_\ell S)$ can be calculated with the expressions of §7.6.b in Landi Degl'Innocenti & Landolfi (2004). These radiative transfer coefficients are proportional to the number density of He 1 atoms, $\mathcal{N}$. Their defining expressions contain also the Voigt profile and the Faraday-Voigt profile (see §5.4 in Landi Degl'Innocenti & Landolfi, 2004), which involve the following parameters: a (i.e., the reduced damping constant), v_{th} (i.e., the velocity that characterizes the thermal motions, which broaden the line profiles), and v_{mac} (i.e., the velocity of possible bulk motions in the plasma, which produce a Doppler shift).

It is important to emphasize that the expressions for the emission and absorption coefficients and those of the statistical equilibrium equations are written in the reference system whose quantization axis is parallel to the magnetic field. The following equation indicates how to obtain the density matrix elements in a new reference system:

$$\left[^{\beta LS}\rho_Q^K(J, J') \right]_{\text{new}} = \sum_{Q'} \left[^{\beta LS}\rho_{Q'}^K(J, J') \right]_{\text{old}} \mathcal{D}_{Q'Q}^K(R)^*, \tag{15}$$

where $\mathcal{D}_{Q'Q}^K(R)^*$ is the complex conjugate of the rotation matrix for the rotation R that carries the old reference system into the new one.

10 Inversion

Our inversion strategy is based on the minimization of a merit function that quantifies how well the Stokes profiles calculated in our atmospheric model reproduce the observed Stokes profiles. To this end, we have chosen the standard χ^2–function, defined as:

$$\chi^2 = \frac{1}{4N_\lambda} \sum_{i=1}^{4} \sum_{j=1}^{N_\lambda} \frac{\left[S_i^{\text{syn}}(\lambda_j) - S_i^{\text{obs}}(\lambda_j) \right]^2}{\sigma_i^2(\lambda_j)}, \tag{16}$$

where N_λ is the number of wavelength points and $\sigma_i^2(\lambda_j)$ is the variance associated to the j-th wavelength point of the i-th Stokes profiles. The minimization algorithm tries to find the value of the parameters of our model that lead to synthetic Stokes profiles S_i^{syn} with the best possible fit to the observations. For our slab model, the number of parameters (number of dimensions of the χ^2 hypersurface) lies between 5 and 7, the maximum value corresponding to the optically thick case. The magnetic field vector (B, θ_B and χ_B), the thermal velocity (v_{th}) and the macroscopic velocity (v_{mac}) are always required. This set of parameters is enough for the case of an optically thin slab. In order to account for radiative transfer effects, we need to define the optical depth of the slab along its normal direction and at a suitable reference wavelength (e.g., the central wavelength of the red blended component for the He I 10830 Å multiplet). In addition, we may additionally need to include the damping parameter (a) of the Voigt profile if the wings of the observed Stokes profiles cannot be fitted using Gaussian line profiles.

10.1   Global Optimization techniques

In order to avoid the possibility of getting trapped in a local minimum of the χ^2 hypersurface, global optimization methods have to be used. We have chosen the DIRECT algorithm (Jones et al., 1993), whose name derives from one of its main features: *di*viding *rect*angles. The idea is to recursively sample parts of the space of parameters, improving in each iteration the location of the part of the space where the global minimum is potentially located. The decision algorithm is based on the assumption that the function is Lipschitz continuous (see Jones et al., 1993, for details). The method works very well in practice and can indeed find the minimum in functions that do not fulfill the condition of Lipschitz continuity. The reason is that the DIRECT algorithm does not require the explicit calculation of the Lipschitz constant but it uses all possible values of such a constant to determine if a region of the parameter space should be broken into subregions because of its potential interest (see Jones et al., 1993, for details).

Since the intensity profile is not very sensitive to the presence of a magnetic field (at least for magnetic field strengths of the order of or smaller than 1000 G), we have decided to estimate the optical thickness of the slab, the thermal and the macroscopic velocity of the plasma and the damping constant by using only the Stokes I profile, and then to determine the magnetic field vector by using the polarization profiles. The full inversion scheme begins by applying the DIRECT method to obtain a first estimation of the indicated four parameters by using only Stokes I. Afterwards, some LM iterations are carried out to refine the initial values of the model's parameters obtained in the previous step. Once the LM method has converged, the inferred values of v_{th}, v_{mac} (together with a and $\Delta\tau$, when these are parameters of the model) are kept fixed in the next steps, in which the DIRECT method is used again for obtaining an initial approximation of the magnetic field vector (B,θ_B,χ_B). According to our experience, the first estimate of the magnetic field vector given by the DIRECT algorithm is typically very close to the final solution. Nevertheless, some iterations of the LM method are performed to refine the value of the magnetic field strength, inclination and azimuth. In any case, although we have found very good results with this procedure, the specific inversion scheme is fully configurable and can be tuned for specific problems.

Our experience has proved that the following strategy is appropriate for inverting prominences. Two initial DIRECT+LM cycles with weights $(1, 0, 0, 0)$ to invert the thermodynamical parameters. Then, two DIRECT+LM cycles in which B, θ_B and χ_B are left free with weights $(0, 0.1, 0.1, 1)$ which tries to set the correct polarity of the field given by Stokes V. An additional LM cycle in which we fit only θ_B and χ_B with the weights $(0, 1, 1, 0.3)$ and a last LM cycle with weights $(0, 0.3, 0.3, 1)$ leaving the full magnetic field vector free.

10.2   Convergence

We let the DIRECT algorithm locate the global minimum in a region whose hypervolume is V. This hypervolume is obtained as the product of the length d_i of each dimension associated with each of the N parameters:

$$V = \prod_i^N d_i. \tag{17}$$

When the hypervolume decreases by a factor f after the DIRECT algorithm has discarded some of the hyperrectangles, its size along each dimension is approximately decreased by a factor $f^{1/N}$. In order to end up with a small region where the global minimum is located, many subdivisions are necessary, thus requiring many function evaluations.

The most time consuming part of any optimization procedure is the evaluation of the merit function. The DIRECT algorithm needs only a reduced number of evaluations of the merit function to find the region where the global minimum is located. For this reason, we have chosen it as the initialization part of the LM method. Since the initialization point is close to the global minimum, the LM method, thanks to its quadratic behavior, rapidly converges to the minimum.

10.3   Stopping criterium

We have used two stopping criteria for the DIRECT algorithm. The first one is stopping when the ratio between the hypervolume where the global minimum is located and the original hypervolume is smaller than a given threshold. This method has been chosen when using the DIRECT algorithm as an initialization for the LM method, giving very good results. The other good option, suggested by Jones et al. (1993), is to stop after a fixed number of evaluations of the merit function.

11   Ambiguities in the Hanle effect in the saturation regime

In the saturation regime of the Hanle effect, Stokes Q and U are insensitive to the field strength, but are sensitive to the geometry of the field. For a $J = 0 \rightarrow J = 1$ transition, the linear polarization can be written as:

$$Q \;=\; \frac{q}{2} \left(3 \cos^2 \theta_B - 1 \right) \sin^2 \Theta_B \cos 2\Phi_B$$

$$U = \frac{q}{2}\left(3\cos^2\theta_B - 1\right)\sin^2\Theta_B \sin 2\Phi_B. \tag{18}$$

These expressions contain a mixture of angles to make it clear that the polarization amplitude depends on both the angle between the vertical and the magnetic field and between the magnetic field and the line-of-sight (LOS).

The coordinates of the magnetic field vector $\mathbf{B}$ in the reference system of the vertical and the reference system of the LOS are:

$$\begin{aligned}
\mathbf{B} &= B\left(\sin\theta_B\cos\phi_B\mathbf{i} + \sin\theta_B\sin\phi_B\mathbf{j} + \cos\theta_B\mathbf{k}\right) \\
\mathbf{B} &= B\left(\sin\Theta_B\cos\Phi_B\mathbf{i}' + \sin\Theta_B\sin\Phi_B\mathbf{j}' + \cos\Theta_B\mathbf{k}'\right),
\end{aligned} \tag{19}$$

where the unit vectors are related by a simple rotation:

$$\begin{aligned}
\mathbf{i}' &= \cos\theta\mathbf{i} - \sin\theta\mathbf{k} \\
\mathbf{k}' &= \sin\theta\mathbf{i} + \cos\theta\mathbf{k}.
\end{aligned} \tag{20}$$

Introducing these relations on the expression for the magnetic field, we find that the following has to be fulfilled, given that the magnetic field vector is the same in both reference systems:

$$\begin{aligned}
\sin\theta_B\cos\phi_B &= \sin\Theta_B\cos\Phi_B\cos\theta + \cos\Theta_B + \sin\theta \\
\sin\theta_B\sin\phi_B &= \sin\Theta_B\sin\Phi_B \\
\cos\theta_B &= \cos\Theta_B\cos\theta - \sin\Theta_B\cos\Phi_B\sin\theta.
\end{aligned} \tag{21}$$

Solving the previous three equations in the two directions, we find the following transformations between the angles in the vertical reference system and the LOS reference system:

$$\begin{aligned}
\cos\Theta_B &= \cos\theta\cos\theta_B + \sin\theta\sin\theta_B\cos\phi_B \\
\sin\Theta_B &= +\sqrt{1 - \cos^2\Theta_B} \\
\cos\Phi_B &= \frac{\cos\theta\sin\theta_B\cos\phi_B - \cos\theta_B\sin\theta}{\sin\Theta_B} \\
\sin\Phi_B &= \frac{\sin\theta_B\sin\phi_B}{\sin\Theta_B}
\end{aligned} \tag{22}$$

and

$$\begin{aligned}
\cos\theta_B &= \cos\theta\cos\Theta_B - \sin\theta\sin\Theta_B\cos\Phi_B \\
\sin\theta_B &= +\sqrt{1 - \cos^2\theta_B} \\
\cos\phi_B &= \frac{\cos\theta\sin\Theta_B\cos\Phi_B + \cos\Theta_B\sin\theta}{\sin\theta_B} \\
\sin\phi_B &= \frac{\sin\Theta_B\sin\Phi_B}{\sin\theta_B}.
\end{aligned} \tag{23}$$

Note that, since $\Theta_B \in [0, \pi]$, we can safely use the square root and take the positive value. In order to transform from one reference system to the other, we can compute the

inclination easily by inverting the sinus or the cosinus. However, the situation is different for the azimuth, because the range of variation is $[-\pi, \pi]$. Therefore, one has to compute the cosinus and the sinus separately and the decide which is the correct quadrant fo the angle in terms of the signs of both quantities.

Four possible kinds of ambiguities can exist for the Stokes Q and U parameters. The idea is that Φ_B can be modified and still obtain the same Q and U by properly adjusting the value of Θ_B. It is clear that, given that the term that can be used to compensate for the change in the azimuth on the LOS reference system is the same for Stokes Q and U, we can only compensate for changes in the sign. Therefore, we have the following potential ambiguities:

$$
\begin{aligned}
\Phi'_B &= \Phi_B \\
\Phi'_B &= \Phi_B - \pi/2 \\
\Phi'_B &= \Phi_B + \pi/2 \\
\Phi'_B &= \Phi_B + \pi.
\end{aligned}
\tag{24}
$$

For each case, we have to compute the value of Θ'_B that keeps the value of Q and U unchanged. Therefore, once we find a solution to the inversion problem in the form of the pair (θ_B, ϕ_B), we can find the remaining solutions in the saturation regime following the recipes that we present now. Remember that, unless one knows the polarity of the field, or in other words, the sign $\cos \Theta_B$, the number of potential ambiguous solutions is 8. If the polarity of the field is known, the number is typically reduced to 4 (or 2 if no 90° ambiguity is present).

12 $\quad \Phi'_B = \Phi_B$

Under this change, we have that

$$
\cos 2\Phi'_B = \cos 2\Phi_B, \quad \sin 2\Phi'_B = \sin 2\Phi_B, \quad \cos \Phi'_B = \cos \Phi_B, \quad \sin \Phi'_B = \sin \Phi_B. \tag{25}
$$

Making use of the previous relations between the angles wrt to the vertical and the LOS, we have to solve the following equation:

$$
\left(3\cos^2 \theta'_B - 1\right) \sin^2 \Theta'_B = \left(3\cos^2 \theta_B - 1\right) \sin^2 \Theta_B, \tag{26}
$$

which can be written as:

$$
\left[3\left(\cos \Theta'_B \cos \theta - \sin \theta \sin \Theta'_B \cos \Phi_B\right)^2 - 1\right] \sin^2 \Theta'_B = \left[3\left(\cos \Theta_B \cos \theta - \sin \theta \sin \Theta_B \cos \Phi_B\right)^2 - 1\right] \sin^2 \Theta_B.
\tag{27}
$$

After some algebra and doing the substitution $t = \sin \Theta'_B$, we end up with the following equation to be solved:

$$
At^4 + Bt^2 + Ct^3 \sqrt{1 - t^2} = K, \tag{28}
$$

where

$$
\begin{aligned}
A &= -3\cos^2 \theta + 3\sin^2 \theta \cos^2 \Phi_B \\
B &= 3\cos^2 \theta - 1 \\
C &= -6\cos \theta \sin \theta \cos \Phi_B \\
K &= \left[3\left(\cos \Theta_B \cos \theta - \sin \theta \sin \Theta_B \cos \Phi_B\right)^2 - 1\right] \sin^2 \Theta_B.
\end{aligned}
\tag{29}
$$

The previous equation can be solved if we make the change of variables $t = \pm\sqrt{Z}$, resulting in:

$$(C^2 + A^2)Z^4 + (-C^2 + 2AB)Z^3 + (-2AK + B^2)Z^2 - 2BKZ + K^2 = 0. \qquad (30)$$

This polynomial of 4-th order can have four different solutions. From these solutions, we have to take only the real solutions which are larger than 0, given the range of variation of Θ_B:

$$t \in \mathbb{R}, \qquad 0 \le t \le 1. \qquad (31)$$

Once the solutions for t are found, we make $\Theta'_B = \arcsin t$. Note that, for a fixed value of t, two values of Θ'_B are possible. We choose the correct one by evaluating the expressions for Q and U and testing which of the two possible choices give the values equal (or very similar) to the original ones.

The angles (θ_B, ϕ_B) are obtained by doing the transformation from (Θ'_B, Φ_B) to the vertical reference system.

13 $\Phi'_B = \Phi_B + \pi$

Under this change, we have:

$$\cos 2\Phi'_B = \cos 2\Phi_B, \quad \sin 2\Phi'_B = \sin 2\Phi_B, \quad \cos \Phi'_B = -\cos \Phi_B, \quad \sin \Phi'_B = -\sin \Phi_B. \qquad (32)$$

Following the same approach, we have to solve for Θ'_B in

$$\left[3 \left(\cos \Theta'_B \cos \theta + \sin \theta \sin \Theta'_B \cos \Phi_B\right)^2 - 1\right] \sin^2 \Theta'_B = \left[3 \left(\cos \Theta_B \cos \theta - \sin \theta \sin \Theta_B \cos \Phi_B\right)^2 - 1\right] \sin^2 \Theta_B. \qquad (33)$$

The solution are obtained as the roots of the same equations as before but now

$$\begin{aligned}
A &= -3\cos^2\theta + 3\sin^2\theta\cos^2\Phi_B \\
B &= 3\cos^2\theta - 1 \\
C &= 6\cos\theta\sin\theta\cos\Phi_B \\
K &= \left[3\left(\cos\Theta_B\cos\theta - \sin\theta\sin\Theta_B\cos\Phi_B\right)^2 - 1\right]\sin^2\Theta_B. \qquad (34)
\end{aligned}$$

The angles (θ_B, ϕ_B) are obtained by doing the transformation from $(\Theta'_B, \Phi_B + \pi)$ to the vertical reference system.

14 $\Phi'_B = \Phi_B + \pi/2$

Under this change, we have:

$$\cos 2\Phi'_B = -\cos 2\Phi_B, \quad \sin 2\Phi'_B = -\sin 2\Phi_B, \quad \cos \Phi'_B = -\sin \Phi_B, \quad \sin \Phi'_B = \cos \Phi_B. \qquad (35)$$

Following the same approach, we have to solve for Θ'_B in

$$\left[3 \left(\cos \Theta'_B \cos \theta + \sin \theta \sin \Theta'_B \sin \Phi_B\right)^2 - 1\right] \sin^2 \Theta'_B = \left[3 \left(\cos \Theta_B \cos \theta - \sin \theta \sin \Theta_B \cos \Phi_B\right)^2 - 1\right] \sin^2 \Theta_B. \qquad (36)$$

The solution are obtained as the roots of the same equations as before but now

$$
\begin{aligned}
A &= -3\cos^2\theta + 3\sin^2\theta\sin^2\Phi_B \\
B &= 3\cos^2\theta - 1 \\
C &= 6\cos\theta\sin\theta\sin\Phi_B \\
K &= -\left[3\left(\cos\Theta_B\cos\theta - \sin\theta\sin\Theta_B\cos\Phi_B\right)^2 - 1\right]\sin^2\Theta_B.
\end{aligned}
\tag{37}
$$

The angles (θ_B, ϕ_B) are obtained by doing the transformation from $(\Theta'_B, \Phi_B + \pi/2)$ to the vertical reference system.

15 $\Phi'_B = \Phi_B - \pi/2$

Under this change, we have:

$$
\cos 2\Phi'_B = -\cos 2\Phi_B, \quad \sin 2\Phi'_B = -\sin 2\Phi_B, \quad \cos\Phi'_B = \sin\Phi_B, \quad \sin\Phi'_B = -\cos\Phi_B.
\tag{38}
$$

Following the same approach, we have to solve for Θ'_B in

$$
\left[3\left(\cos\Theta'_B\cos\theta + \sin\theta\sin\Theta'_B\sin\Phi_B\right)^2 - 1\right]\sin^2\Theta'_B = \left[3\left(\cos\Theta_B\cos\theta - \sin\theta\sin\Theta_B\cos\Phi_B\right)^2 - 1\right]\sin^2\Theta_B.
\tag{39}
$$

The solution are obtained as the roots of the same equations as before but now

$$
\begin{aligned}
A &= -3\cos^2\theta + 3\sin^2\theta\sin^2\Phi_B \\
B &= 3\cos^2\theta - 1 \\
C &= -6\cos\theta\sin\theta\sin\Phi_B \\
K &= -\left[3\left(\cos\Theta_B\cos\theta - \sin\theta\sin\Theta_B\cos\Phi_B\right)^2 - 1\right]\sin^2\Theta_B.
\end{aligned}
\tag{40}
$$

The angles (θ_B, ϕ_B) are obtained by doing the transformation from $(\Theta'_B, \Phi_B - \pi/2)$ to the vertical reference system.

Acknowledgements

References

Belluzzi, L., Trujillo Bueno, J., & Landi Degl'Innocenti, E. 2007, ApJ, 666, 588

Condon, E. U., & Shortley, G. H. 1935, The Theory of Atomic Spectra (Cambridge: Cambridge University Press)

Edmonds, A. R. 1960, Angular Momentum in Quantum Mechanics (Princeton University Press)

Jones, D. R., Perttunen, C. D., & Stuckmann, B. E. 1993, Journal of Optimization Theory and Applications, 79, 157

Landi Deglinnocenti, E., & Landi Deglinnocenti, M. 1985, Sol. Phys., 97, 239

Landi Degl'Innocenti, E., & Landolfi, M. 2004, Polarization in Spectral Lines (Kluwer Academic Publishers)

Pierce, K. 2000, in Allen's Astrophysical Quantities, ed. A. N. Cox (New York: Springer Verlag and AIP Press)

Rees, D. E., Durrant, C. J., & Murphy, G. A. 1989, ApJ, 339, 1093

Trujillo Bueno, J. 2003, in Stellar Atmosphere Modeling, ed. I. Hubeny, D. Mihalas, & K. Werner, ASP Conf. Ser. 288 (San Francisco: ASP), 551

Trujillo Bueno, J., & Asensio Ramos, A. 2007, ApJ, 655, 642

Trujillo Bueno, J., Merenda, L., Centeno, R., Collados, M., & Landi Degl'Innocenti, E. 2005, ApJ, 619, L191